Table 3 ISSVA classification of vascular tumors and malformations

Vascular tumors	Vascular malformations	
Infantile hemangiomas	Slow-flow	Capillary malformation (CM)
Congenital hemangiomas (RICH and NICH)		Port-wine stain
Tufted angioma		Telangiectasia
Kaposiform hemangioendothelioma		Angiokeratoma
Spindle cell hemangioendothelioma		Venous malformation (VM)
Other, rare hemangioendotheliomas (epithelioid, composite, retiform, polymorphous, Dabska tumor, lymphangioendotheliomatosis, etc.)		Common sporadic (VM)
Dermatologic acquired vascular tumors (pyogenic granuloma, targetoid hemangioma, glomeruloid hemangioma, microvenular hemangioma, etc.)		Bean syndrome
		Familial cutaneous and mucosal Venous malformation (VMCM)
		Glomuvenous malformation (GVM) (Glomangioma)
		Maffucci syndrome
		Lymphatic malformation (LM)
	Fast-flow	Arterial malformation (AM)
		Arteriovenous fistula (AVF)
		Arteriovenous malformation (AVM)
	Complex-combined	CVM, CLM, LVM,CLVM, AVM-LM, CM-AVM

Table 4 ISSVA classification versus classical classification

ISSVA classification	Classical classification (including WHO classification)
Vascular tumors	
Infantile hemangioma	Strawberry mark (Cherry hemangioma)
	Hemangioma of infancy
	Capillary hemangioma
Congenital hemangioma	Strawberry mark (Cherry hemangioma)
	Hemangioma of infancy
	Capillary hemangioma
Vascular malformation (High-flow)	
Arteriovenous malformation (AVM)	Arteriovenous hemangioma
Vascular malformation (Slow-flow)	
Venous malformation (VM)	Cavernous hemangioma
	Venous hemangioma
	Intramuscular hemangioma
Capillary malformation (CM)	Port-wine stain
	Hemangioma simplex
	Angiokeratoma
Lymphatic malformation (LM)	Lymphangioma, cystic hygroma, cavernous lymphangioma

approximately to "strawberry mark", "hemangioma of infancy" and "capillary hemangioma" in the WHO classification (Table 4).

Infantile hemangioma (IH)

Infantile hemangioma is the most common benign tumor in neonates and infants. It has a characteristic clinical course in which it rapidly grows after birth (several days to a few weeks after birth) until 12–18 months of age, and then slowly regresses over several years. The former is called "the proliferative phase" and the latter is called "the involuting phase." It is commonly known as a "strawberry mark," the term used in the WHO classification. Histopathologically, it is characterized by positive glucose transporter-1 (GLUT-1) staining. Although superficial lesions are diagnosed easily, diagnostic imaging is required for lesions in deep tissues and intractable alarming hemangioma involving the orbit or the respiratory tract. Interest in this disease has recently increased because it has been reported that beta blockers are highly effective against IH [3].

Imaging findings are different between the proliferative phase and the involuting phase [4]. In the proliferative phase, the pathological findings are the proliferation of vascular endothelial cells and the lobulated mass of tissues, which results in a sharply marginated hypervascular mass radiographically. Low to high echogenicity are observed on ultrasound images and arterial blood flow is seen on color Doppler images (Fig. 1a). On MRI, IHs are well-circumscribed, lobulated masses with isointensity or low intensity on T1-weighted images (Fig. 1b) and relatively uniform

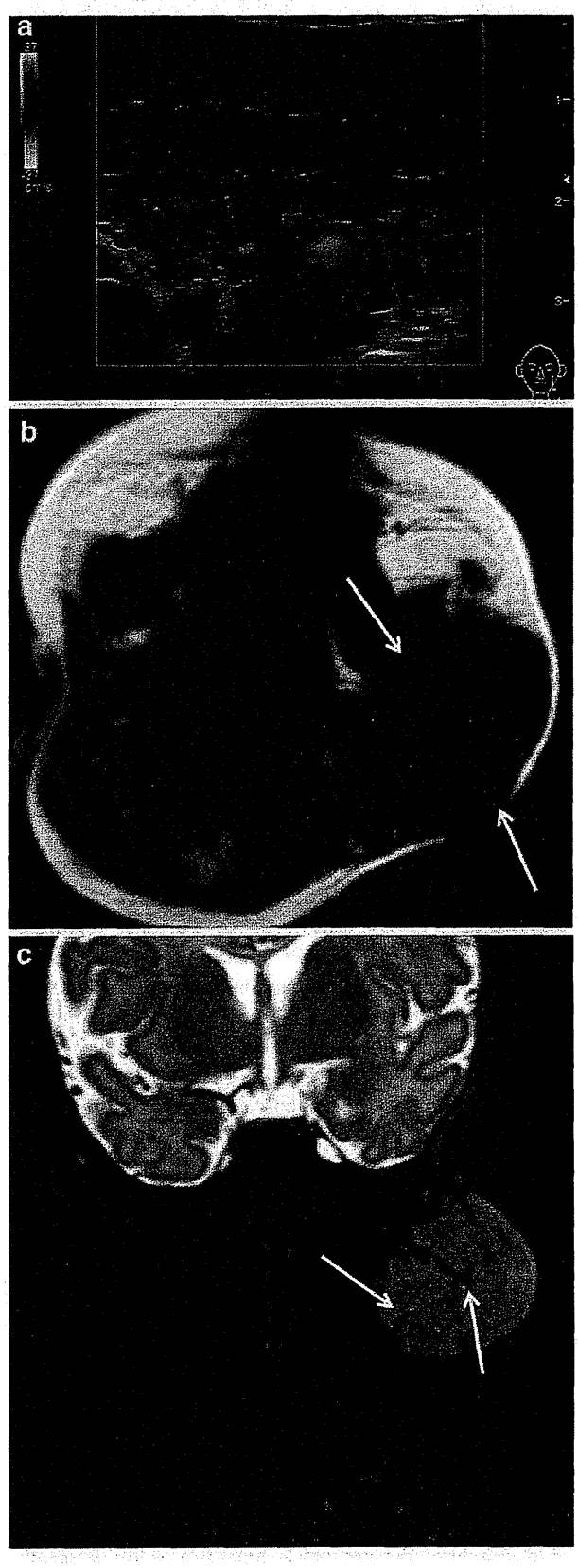

◀ **Fig. 1** Infantile hemangioma in the proliferative phase on the cheek of a 13-month-old boy. **b** Axial T1-weighted MR image shows a well-defined mass, isointense to muscle (*arrows*). **c** Coronal fat-saturated T2-weighted MR image of the neck shows high intensity to muscle with flow voids (*arrows*). **a** Color Doppler US demonstrates arterial flow within a mass

high intensity, with flow voids reflecting arterial blood flow on T2-weighted images and fat suppressed (FS) T2-weighted images (Fig. 1c). On contrast-enhanced MRI, there is vivid staining in the early phase and the staining is maintained until the delayed phase. In the involuting phase, vascular endothelial cells pathologically decrease through apoptosis and are then replaced by fibro-fatty tissues. Reflecting this, decreased arterial blood flow and fat displacement are observed on images (Fig. 2).

Congenital hemangioma (CH)

Congenital hemangioma was first reported by Boon et al. [5] in 1996 as IH-like lesions that presented the peak proliferation or were regressing at birth. It is classified into two types: rapidly involuting CH (RICH), which achieves a complete regression by approximately 12–14 months after birth, and non-involuting CH (NICH), which may partially

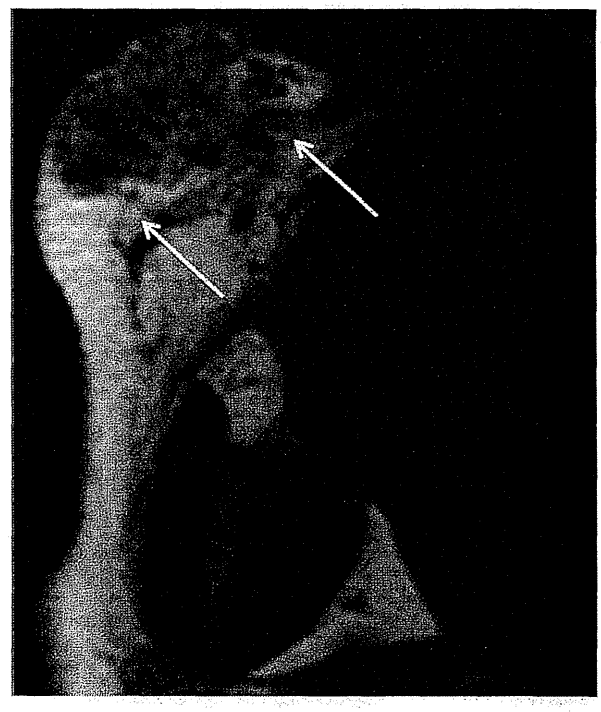

Fig. 2 Infantile hemangioma in the involuting phase on the right mandible of a 2-year-old boy who received laser treatment. Axial T1-weighted MR image shows a mass including loose fibrofatty tissue (*arrows*)

grow but does not regress. Unlike IH, immunostaining with GLUT-1 is negative in vascular endothelial cells. The incidence of CH is unknown but is believed to be low, and the incidence of NICH is believed to be lower than that of RICH. It is difficult to clinically distinguish between RICH and NICH at a given time point, and it is important to monitor the clinical course.

There have been few reports on imaging findings [6, 7]. Imaging findings on CH are basically similar to those on IH, and arterial blood flow is also seen in the mass (Fig. 3a–c). Unlike IH, CH tends to show inhomogeneous parenchyma in the mass with poor margins on ultrasound and MR images and it sometimes shows calcification (Fig. 4a–g). In angiography, aneurysm formation with AV shunt and venous dilatation tend to be obvious.

Kaposiform hemangioendothelioma (KHE)/tufted angioma (TA)

Kaposiform hemangioendothelioma was first reported by Zukerberg et al. [8] in 1993 as a Kaposi's sarcoma-like tumor that occurred in infants. KHE has been reported to occur in infants at birth and aged 10 years and younger in many cases, and reports on adult cases have been increasing recently. It is a locally invasive tumor showing progressive proliferation of vascular endothelial cells with poor margins. It sometimes invades the muscle and bone [9].

Today, tufted angioma is believed to be a subtype of KHE, and is a tumor showing intradermal proliferation of vascular endothelial cells in clusters called "cannon balls." It often develops on the skin and rarely requires diagnostic

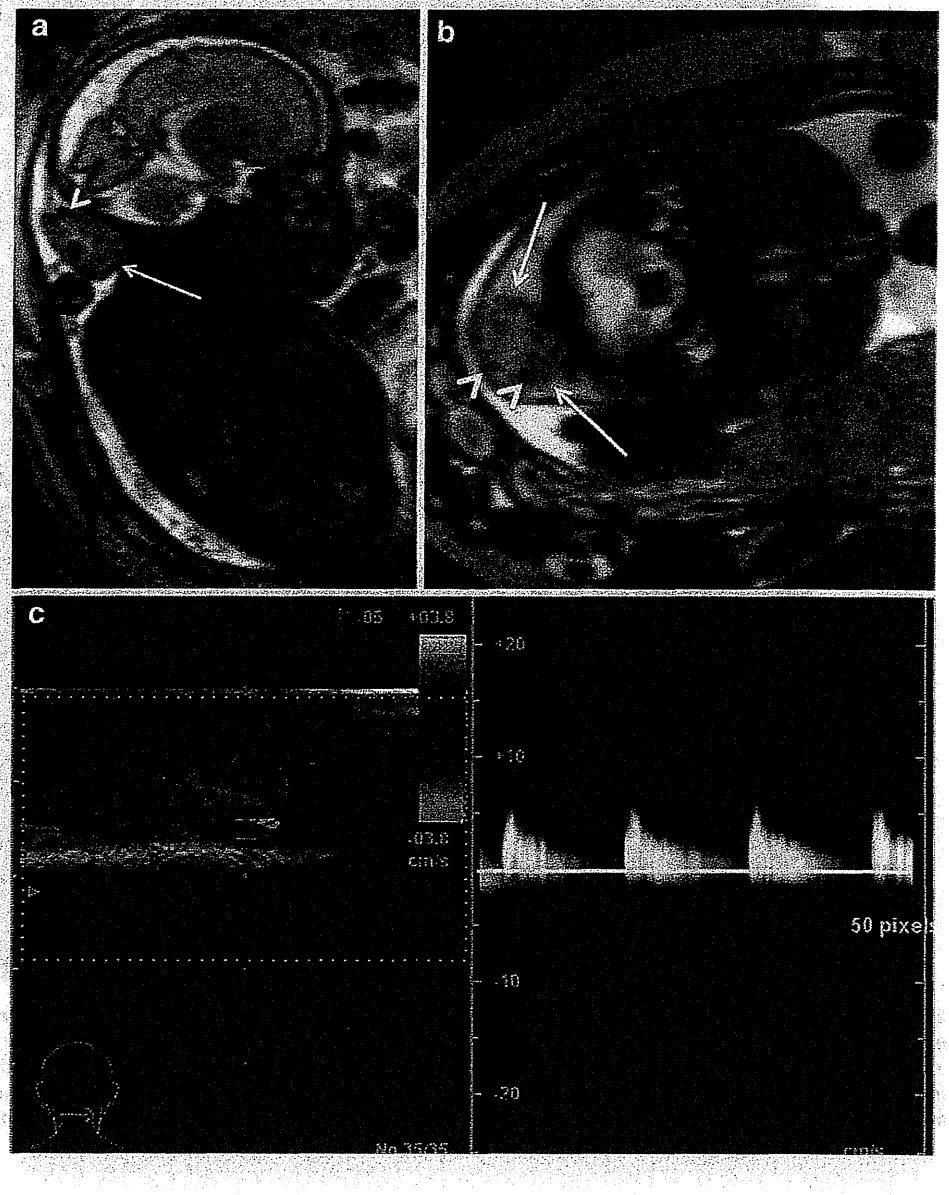

Fig. 3 Rapidly involuting congenital hemangioma (RICH) involving the posterior cervical region. **a**, **b** Sagittal and axial fetal MR images on single-shot FSE sequence show well-defined subcutaneous mass (*arrows*) with flow voids (*arrowheads*) at 29 weeks gestation. **c** Color Doppler US shows arterial flow in the mass. The lesion demonstrated significant involution in 6 months

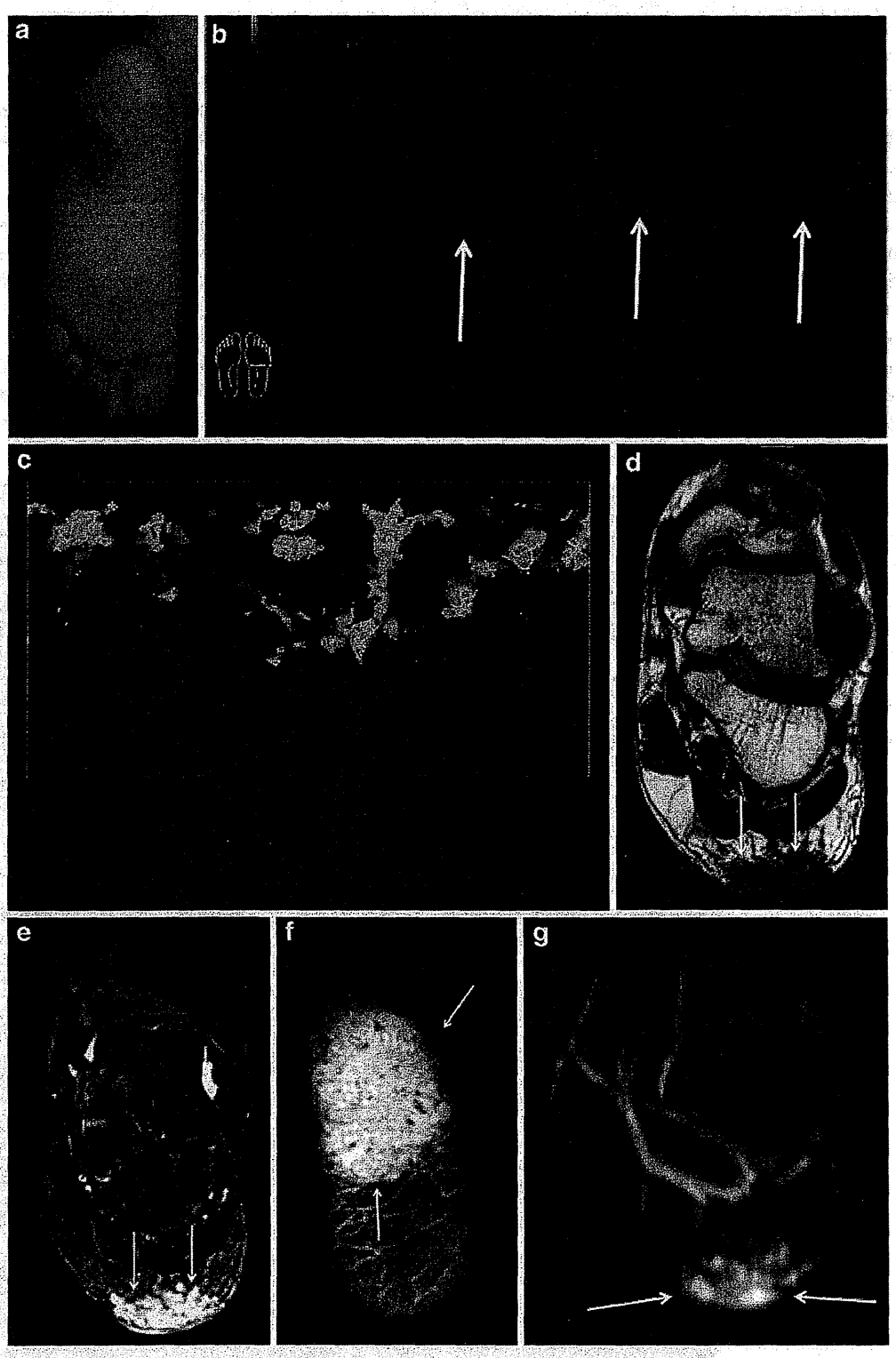

Fig. 4 Non-involuting congenital hemangioma (NICH) in the left sole. **a** A soft-tissue mass with reddish discoloration present since birth in a 12-year-old boy. **b** US shows ill-defined heterogeneous plantar solid mass (*arrows*). **c** Color Doppler US shows hypervascular mass with arterial flow. **d** Coronal T1-weighted MR image shows an ill-defined mass isointense to muscle (*arrows*). **e** Coronal fat-saturated T2-weighted MR image shows high intensity to muscle (*arrows*). **f** Axial fat-saturated contrast-enhanced T1-weighted MR image shows vivid enhancement of the lesion (*arrows*). **g** Time-resolved MR angiogram shows prominent enhancement in the arterial phase (*arrows*)

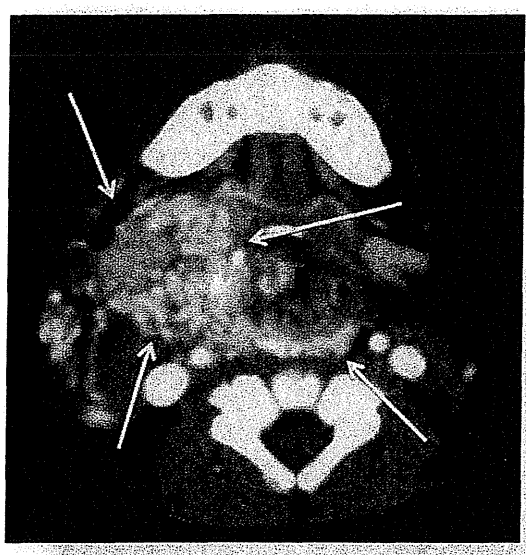

Fig. 5 Kaposiform hemangioendothelioma in a 2-month-old boy with Kasabach–Meritt syndrome. Axial contrast-enhanced CT image shows an ill-defined mass with prominent enhancement in the arterial phase (*arrows*)

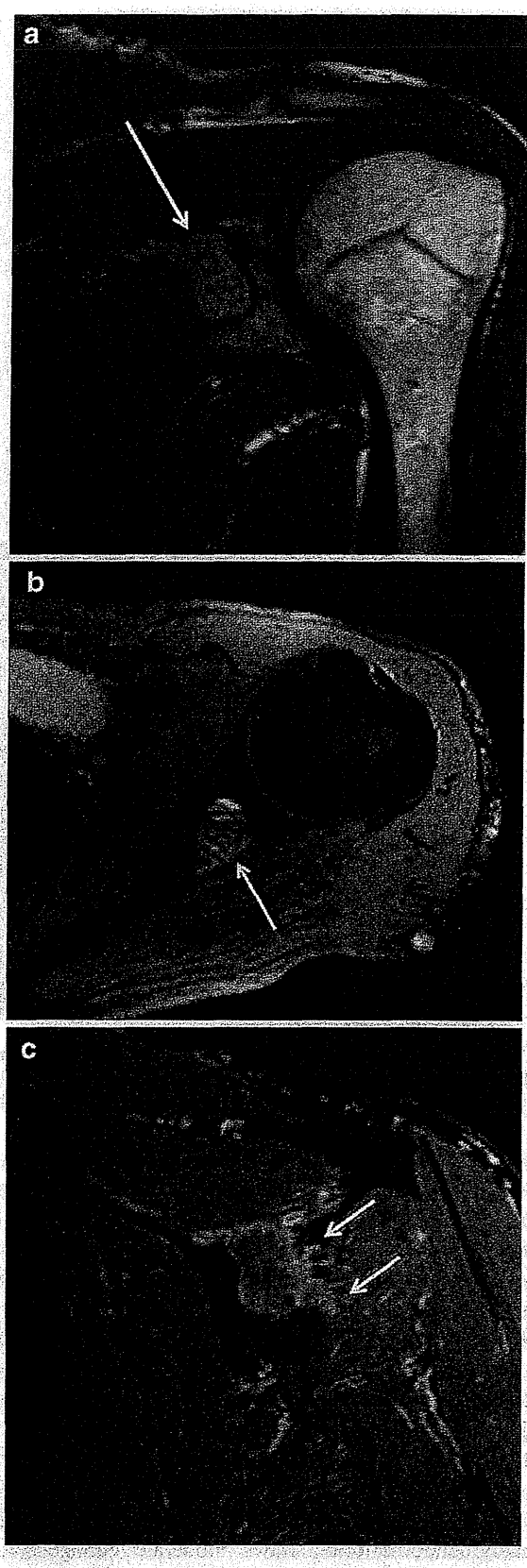

Fig. 6 Retiform hemangioendothelioma in a 42-year-old woman who presented with left shoulder pain. She had undergone several surgical operations for local recurrence from childhood. **a** Coronal T1-weighted MR image shows a slight, ill-defined mass near the suprascapular notch, hyperintense to muscle (*arrow*). **b** Axial fat-saturated T2-weighted MR image shows intermediate intensity to muscle (*arrow*). **c** Coronal contrast-enhanced T1-weighted MR image shows a heterogeneous, ill-defined mass with proliferation of vascular channels of peripheral area (*arrows*)

imaging, and is considered to be the same lesion as angioblastoma (Nakagawa) [10] in Japan. It is now believed that KHE and TA cause Kasabach–Merritt syndrome [11].

On diagnostic imaging, it is characteristically seen as hypervascular invasive tumors with poor margins [12] (Fig. 5). On MRI, KHE/TA typically appears as ill-circumscribed masses with low or isointensity areas on T1-weighted images and high intensity on T2-weighted images. On contrast-enhanced MRI, it often shows inhomogeneous staining. Similar tendencies are observed on ultrasound images, which show poorly-marginated hypervascular lesions with low to high echogenicity.

Other, rare hemangioendotheliomas

Hemangioendothelioma is a vascular tumor of borderline malignancy that develops from vascular endothelial cells, and is positioned between hemangioma (benign) and angiosarcoma (malignant). The subtypes include epithelioid, retiform, composite, pseudomyogenic and papillary intralymphatic angioendothelioma. The assignment of the

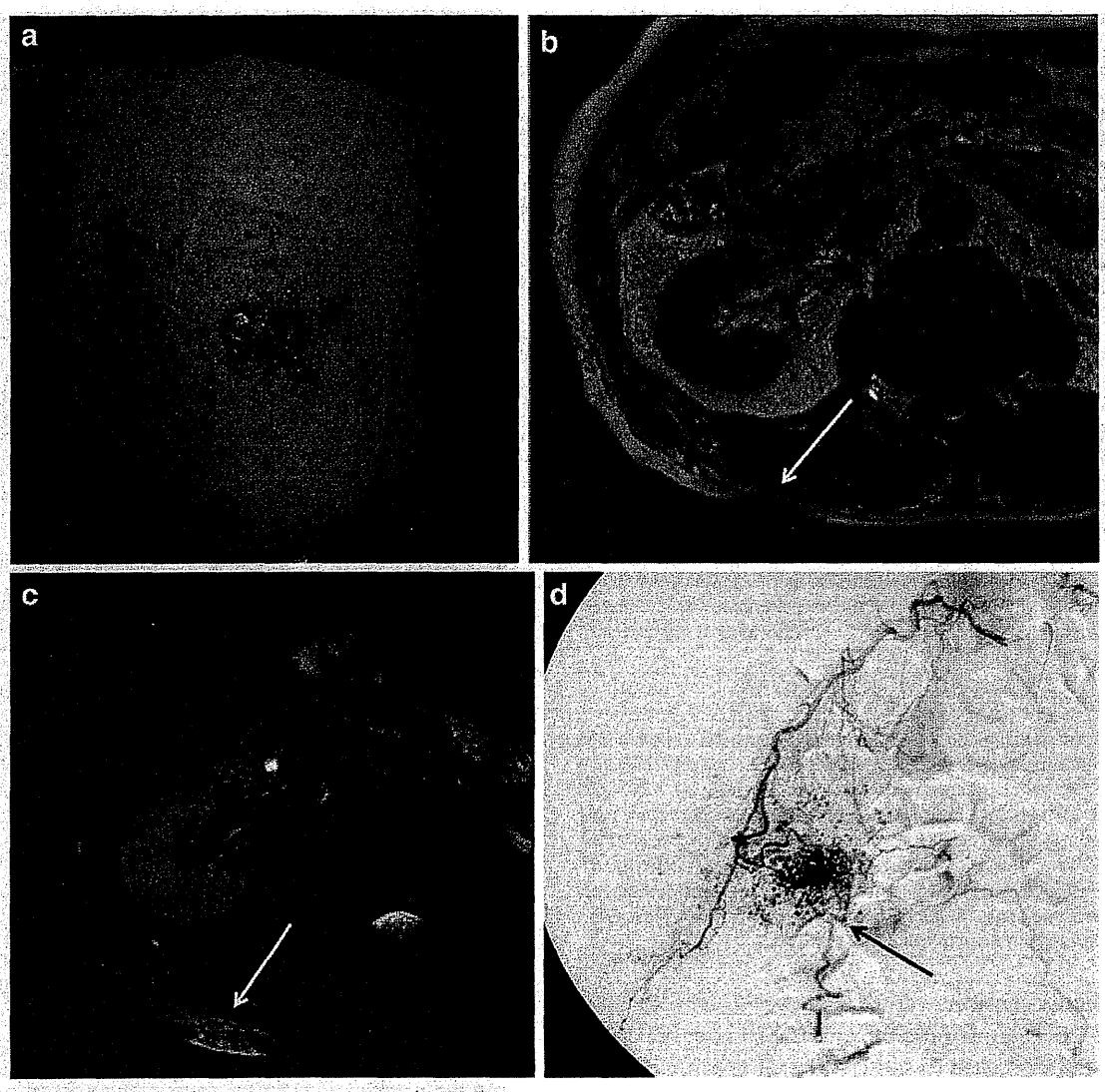

Fig. 7 Pyogenic granuloma of the back in a 66-year-old man. **a** Clinical image shows multiple reddish papules. **b** Axial T1-weighted MR image shows a homogeneous mass isointense to muscle (*arrow*). **c** Axial fat-saturated T2-weighted MR image shows high intensity to muscle (*arrow*). **d** Angiography shows ill-defined prominent enhancement area (*arrow*)

term used for hemangioendothelioma was problematic because it was used for different types, including benign, borderline malignant and malignant tumors, resulting in confusion in the past. Now it is generally used to mean a tumor of borderline malignancy, except for epithelioid hemangioendothelioma.

Hemangioendothelioma includes superficial tumors that occur on or under the skin and tumors that occur in deep tissues such as muscles. Each type has different imaging findings in general [13].

Superficial lesions involve thickening of the skin and subcutaneous tissues, and often form localized masses. Characteristics in lesions are non-specific. Hemangioendothelioma shows moderate echogenicity on ultrasound images. On MRI, the mass shows isointensity on T1-weighted images and iso or high intensity on T2-weighted images. The proliferation and dilation of the vascular channels are not obvious in many cases.

In contrast, deep lesions show obvious proliferation of vascular components compared to other soft tissue masses, and AV shunts are identifiable. On ultrasound images, although the echogenicity of masses are various (low to high echogenicity), bleeding is seen as a cystic change and AV shunts are identified on color Doppler images. On MRI, although they show non-specific findings of isointensity areas on T1-weighted images and high intensity areas on T2-weighted images, an obvious enhancement is seen in the early phase on MRI with gadolinium (Gd), reflecting the proliferation of vascular channels (Fig. 6a–c).

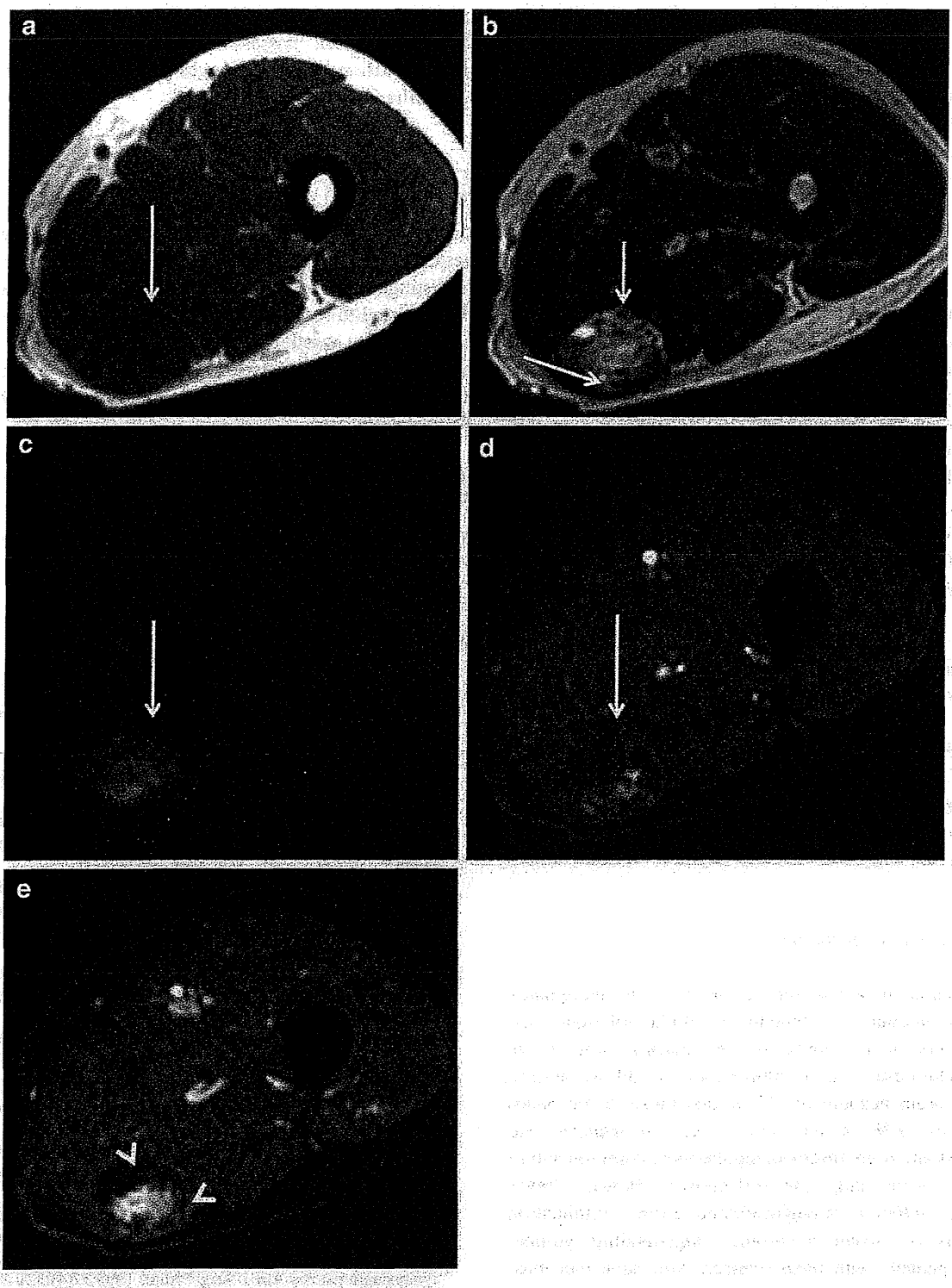

Fig. 8 Angiosarcoma of soft tissue in a 50-year-old female in the thigh. **a** Axial T1-weighted MR image shows a well-defined mass in the hamstring, isointense to muscle (*arrow*). **b** Axial T2-weighted MR image shows a heterogeneous signal with flow voids (*arrows*). **c** Diffusion-weighted MR image demonstrates diffusion restriction (*arrow*). **d**, **e** Axial contrast-enhanced T1-weighted MR image shows gradual enhancement from arterial phase (*arrow*) to venous phase (*arrowheads*)

Dermatologic acquired vascular tumors

These are vascular tumors that are skin lesions and are rarely examined through diagnostic imaging. In this paper, a description is provided only on pyogenic granuloma, which is sometimes found as a subcutaneous mass.

Pyogenic granuloma

Pyogenic granuloma was first reported by Poncet and Dor [14] in 1897. Despite its name, it is not a granuloma but a vascular tumor. It is a protruded lesion with hemorrhagic tendencies that occurs on the skin or mucosa. It often causes ulcers to have a granulation tissue-like appearance and it appears to be pyogenic because of secondary infections and exudative change; and for these reasons it is named "pyogenic granuloma" [15]. The etiology is not clear, and the involvement of local factors such as trauma, infection, and chronic stimulation is suspected. Favorite sites include the areas for cervicofacial and oral surgery and for dermatology, but it sometimes occurs in the gastrointestinal tract or other sites.

There are no detailed reports on imaging findings. Pyogenic granuloma is a sharply marginated mass with slightly high echogenicity on ultrasound images, and shows high flow on color Doppler images. On MRI, when compared to the muscle, the mass shows isointensity on T1-weighted images and high intensity on T2-weighted images and FS-T2-weighted images (Fig. 7a–d). Some case reports (including intravenous variants) state that many pyogenic granulomas are generally highly enhanced in contrast enhanced CT and MRI because they are vascular tumors [16, 17].

Angiosarcoma of soft tissue

Angiosarcoma is a vascular tumor of high malignancy involving vascular and lymphatic cellular elements and often occurs on and under the cervicofacial skin in the elderly [18]. Lesions in the skin account for 33 %, those in the soft tissues account for 23 %, and those in the bones account for 6 % of the total. Local recurrences and metastases are often observed and the most common site of metastasis is the lung. The well-known "Stewart–Treves syndrome" refers to an angiosarcoma, a rare complication that forms as a result of chronic, long-standing lymphedema in patients with breast cancer, who have had mastectomy and/or radiotherapy.

On MRI, it shows non-specific imaging findings of isointensity on T1-weighted images and high intensity on T2-weighted images and FS-T2-weighted images. The mass shows prominent enhancement with Gd, and is characterized by obvious vascular proliferation; in particular, vascular proliferation is often seen along the periphery of such masses. Because of high tumor cellularity, diffusion-weighted images generally show diffusion restriction [19] (Fig. 8a–e).

Conclusion

Although vascular tumors are generally handled as suggested by their traditional term, "hemangioma", it is useful to distinguish tumors requiring treatment from those that are expected to spontaneously regress and only have to be followed up, based on the ISSVA classification. It is essential for radiologists to become familiar with clinical and imaging findings on vascular tumors based on the ISSVA classification.

Acknowledgments The authors thank Jay Starkey, MD for valuable assistance in manuscript preparation.

Conflict of interest The authors declare that they have no conflict of interest.

References

1. Fletcher CDM, Bridge JA, Hogendoorn PCW, Mertens F. Vascular tumors, WHO classification of tumors of soft tissue and bone. 4th ed. Lyon: IARC Press; 2013. p. 137–58.
2. Enjolras O. Classification and management of the various superficial vascular anomalies: hemangiomas and vascular malformations. J Dermatol. 1997;24(11):701–10.
3. Léauté-Labrèze C, Dumas de la Roque E, Hubiche T, Boralevi F, Thambo JB, Taïeb A. Propranolol for severe hemangiomas of infancy. N Engl J Med. 2008;358(24):2649–51.
4. Restrepo R, Palani R, Cervantes LF, Duarte AM, Amjad I, Altman NR. Hemangiomas revisited: the useful, the unusual and the new. Part 1: overview and clinical and imaging characteristics. Pediatr Radiol. 2011;41(7):895–904.
5. Boon LM, Enjolras O, Mulliken JB. Congential hemangioma: evidence of accelerated involution. J Pediatr. 1996;128(3):329–35.
6. Gorincour G, Kokta V, Rypens F, Garel L, Powell J, Dubois J. Imaging characteristics of two subtypes of congenital hemangiomas: rapidly involuting congenital hemangiomas and non-involuting congenital hemangiomas. Pediatr Radiol. 2005;35(12):1178–85.
7. Fadell MF 2nd, Jones BV, Adams DM. Prenatal diagnosis and postnatal follow-up of rapidly involuting congenital hemangioma (RICH). Pediatr Radiol. 2011;41(8):1057–60.
8. Zukerberg LR, Nickoloff BJ, Weiss SW. Kaposiform hemangioendothelioma of infancy and childhood. An aggressive neoplasm associated with Kasabach-Merritt syndrome and lymphangiomatosis Am J Surg Pathol. 1993;17(4):321–8.
9. Gruman A, Liang MG, Mulliken JB, Fishman SJ, Burrows PE, Kozakewich HP, et al. Kaposiform hemangioendothelioma without Kasabach-Merritt phenomenon. J Am Acad Dermatol. 2005;52(4):616–22.
10. Cho KH, Kim SH, Park KC, Lee AY, Song KY, Chi JG, et al. Angioblastoma (Nakagawa)—is it the same as tufted angioma? Clin Exp Dermatol. 1991;16(2):110–3.

11. Nozaki T, Nosaka S, Miyazaki O, Makidono A, Yamamoto A, Niwa T, et al. Syndromes associated with vascular tumors and malformations: a pictorial review. Radiographics. 2013;33(1): 175–95.
12. Tamai N, Hashii Y, Osuga K, Chihara T, Morii E, Aozasa K, et al. Kaposiform hemangioendothelioma arising in the deltoid muscle without the Kasabach-Merritt phenomenon. Skeletal Radiol. 2010;39(10):1043–6.
13. Kransdorf MJ, Murphey MD. Imaging of soft tissue tumors. 2nd ed. Philadelphia: Lippincott Williams & Wilkins; 2006. p. 177–85.
14. Poncet A, Dor L. Botryomycose humaine. Rev Chir Orthop. 1897;18:996–7.
15. Weiss SW, Goldblum JR. Benign tumors and tumor-like lesions of blood vessels. In: Weiss SW, Goldblum JR, editors. Enzinger and Weiss's soft tissue tumors. St. Louis: Mosby; 2001. p. 837–915.
16. Kamishima T, Hasegawa A, Kubota KC, Oizumi N, Iwasaki N, Minami A, et al. Intravenous pyogenic granuloma of the finger. Jpn J Radiol. 2009;27(8):328–32.
17. Lee G, Suh K, Lee Y, Kang I. CT findings in two cases of lobular capillary haemangioma of the nasal cavity: focusing on the enhancement pattern. Dentomaxillofac Radiol. 2012;41(2):165–8.
18. Walker EA, Salesky JS, Fenton ME, Murphey MD. Magnetic resonance imaging of malignant soft tissue neoplasms in the adult. Radiol Clin N Am. 2011;49(6):1219–34.
19. Murphey MD, Fairbairn KJ, Parman LM, Baxter KG, Parsa MB, Smith WS. From the archives of the AFIP. Musculoskeletal angiomatous lesions: radiologic-pathologic correlation. Radiographics. 1995;15(4):893–917.

Preliminary Experience With Intraoperative Near-infrared Fluorescence Imaging in Percutaneous Sclerotherapy of Soft-Tissue Venous Malformations

KOSUKE ISHIKAWA, MD,* SATORU SASAKI, MD, PHD,* HIROSHI FURUKAWA, MD, PHD,† MUNETOMO NAGAO, MD, PHD,* DAISUKE IWASAKI, MD,* NORIKO SAITO, MD, PHD,* AND YUHEI YAMAMOTO, MD, PHD†

BACKGROUND It has recently been demonstrated that near-infrared (NIR) fluorescence imaging can be used to visualize the blood vasculature. Although sclerotherapy has been successfully used in treating venous malformations, the spread of sclerosant is difficult to monitor during sclerotherapy.

OBJECTIVE To evaluate the safety and efficacy of NIR fluorescence imaging in percutaneous sclerotherapy of soft-tissue venous malformations.

METHODS AND MATERIALS The use of NIR fluorescence imaging after administration of indocyanine green (ICG) was evaluated in duplex-guided sclerotherapy performed on 15 patients with venous malformations. The lower extremities were involved in seven, the upper extremities in four, and the face in four.

RESULTS In 13 of the 15 procedures, spotty fluorescence images were obtained, and in eight procedures, linear fluorescence images were obtained. In two patients with intramuscular venous malformations in the lower extremities, no fluorescence images were obtained. Observational depth seemed to be <1 cm below the skin surface with an ICG concentration of 0.01 mg/mL. No complications associated with ICG were observed. Adjacent tissue ulceration occurred in one patient.

CONCLUSION NIR fluorescence imaging with ICG can be a useful additional monitor for percutaneous sclerotherapy of venous malformations, especially in the face and hands, enabling noninvasive assessment of real-time spread of sclerosant.

The authors have indicated no significant interest with commercial supporters.

Sclerotherapy has been a useful alternative to surgical excision of vascular malformations.[1,2] One of the most common causes of complications during the procedure is extravasation of sclerosant, with necrosis of adjacent tissue.[3] Therefore, procedural guidance is required to ensure precise puncture, and the spread of sclerosant should be carefully monitored. Various sclerotherapy techniques have been reported: fluoroscopic guided,[3] duplex guided,[4] and magnetic resonance (MR) guided.[5] Recently near-infrared (NIR) fluorescence imaging has been demonstrated to offer real-time visualization, enabling noninvasive assessment of lymphatic and blood vasculature.[6] Kikuchi and Hosokawa reported that intraoperative NIR fluorescence imaging allowed for visualization of sclerosant spreading in varicose veins.[7] We used a real-time NIR fluorescence imaging system with indocyanine green (ICG) as an additional monitor of the spread of sclerosant in duplex-guided percutaneous sclerotherapy of soft-tissue venous malformations. In this report, we describe our clinical experience and evaluate the safety and efficacy of NIR fluorescence imaging.

Center for Vascular Anomalies, KKR Sapporo Medical Center Tonan Hospital, Sapporo, Japan; †Department of Plastic and Reconstructive Surgery, Hokkaido University Graduate School of Medicine, Sapporo, Japan

ISSN: 1076-0512 • Dermatol Surg 2013;39:907–912 • DOI: 10.1111/dsu.12152

Patients

The use of NIR fluorescence imaging was evaluated in duplex-guided percutaneous sclerotherapy performed on 15 patients (ages 3–64, average 14.9) with venous malformations from March to August 2010 at KKR Sapporo Medical Center Tonan Hospital. The lower extremities were involved in seven, the upper extremities in four, and the face in four. Before the procedure, all patients underwent color duplex ultrasound and MR imaging to evaluate the extent, distribution, and character of the lesions. The diagnosis of a venous malformation was made on the basis of clinical history, physical examination, ultrasound, and MR imaging. The lesions of all patients in the study met the MR imaging criteria for venous malformations.[8] Follow-up ranged from 1 to 16 months (average 6.3 months). This study conformed to the ethical guidelines of the 1975 Declaration of Helsinki.

Methods

NIR Fluorescence Imaging

Intraoperatively, venous malformations were visualized through direct injection of a solution of ICG and sclerosant using a NIR fluorescence camera device [Photodynamic Eye (PDE); Hamamatsu Photonics K.K., Shizuoka, Japan] equipped with 760-nm light-emitting diodes within a handheld unit with a charge-coupled device camera as a detector and a bandpass filter to block light below 820 nm.[6] The maximum excitation and fluorescence wavelengths of ICG in plasma are 765 nm and 840 nm, respectively.[9] Fluorescence within the NIR spectral range ($\geq$ 800 nm) is tissue penetrating, and the PDE provides noninvasive detection of the fluorescence in deeper tissues. This device is portable and easy to use intraoperatively. The fluorescence signals were digitalized for real-time display in monochrome. According to the recorded movies of the procedures, patterns of fluorescence images were classified as linear images, spotty images, or no images obtained. Linear images were defined as more than one vessel-like fluorescence pattern originating from spotty images, which were defined as a local dim fluorescence pattern.

ICG and Sclerosants

ICG (Diagnogreen for injection; Daiichi-Sankyo Co. Ltd., Tokyo, Japan) was used as an NIR fluorophore. Concentrated ICG solution (0.04 mL) was made by dissolving ICG (25 mg) in injection solvent (10 mL) and added to 10 mL of sclerosant solution, resulting in an ICG concentration of 0.01 mg/mL.[7] The sclerosants were absolute ethanol and 3% polidocanol (Polidocasklerol 3% injection; Zeria Pharmaceutical Co., Ltd., Tokyo, Japan) foamed using the Tessari method.[10] The stable sclerosing microfoam was obtained by mixing 2 mL of polidocanol with atmospheric air at a 1:4 ratio in two syringes attached using a three-way stopcock.

Procedures

All patients were treated under general anesthesia. Direct puncture of the venous malformation was performed using a 22-G angiocatheter with color duplex ultrasound (LOGIQ e; GE Yokogawa Medical Co., Ltd., Tokyo, Japan) to visualize needle placement and facilitate direct cannulation of the vascular channels. Then sclerosant solution mixed with ICG was slowly injected under duplex guidance, and fluorescence images were obtained through the PDE held 15–20 cm from the skin surface to monitor the spread of sclerosant. Operating lights were turned off during the procedure, and room lights were left on to keep light reflection off the skin. In most patients, direct puncture and sclerosis were performed in more than one region of the venous malformation. The sclerotherapy was stopped when the vascular lesion was sufficiently filled according to duplex sonography, when the use of sclerosants reached a maximum dose of 1 mL/kg, or when fluorescence images were obtained at the contralateral side of the treated finger.

Results

Patient characteristics, treatments, and outcomes are summarized in Table 1. Spotty fluorescence images

TABLE 1. Patient Characteristics, Treatments and Outcomes

Patient			Venous Malformation				
No.	*Age*	*Sex*	*Location*	*Distribution*	*Treated region*	*Sclerosant*	*Pattern of Fluorescence Images*
1	7	Male	SC	Upper extremity	Hand	POL	Linear
2	17	Male	SC	Face	Lip	ET	Spotty
3	11	Male	IM	Lower extremity	Thigh	ET	None obtained
4	7	Female	SC	Lower extremity	Thigh	ET	Spotty
5	15	Female	SC	Lower extremity	Thigh, buttock	ET	Linear
6	11	Female	SC	Lower extremity	Buttock	ET, POL	Spotty
7	17	Female	IM	Lower extremity	Leg	ET	None obtained
8	6	Female	SC	Upper extremity	Fingers	POL	Linear
9	11	Female	SC	Face	Cheek	ET	Linear
10	17	Female	SC	Upper extremity	Thumb	ET	Linear
11	9	Male	SC	Lower extremity	Leg	POL	Spotty
12	3	Male	SC	Lower extremity	Foot	ET, POL	Spotty
13	64	Female	SC	Face	Lower eyelid	POL	Linear
14	6	Female	SC	Upper extremity	Finger	POL	Linear
15	22	Female	SC	Face	Lip	ET, POL	Linear

SC, subcutaneous; IM, intramuscular; POL, polidocanol; ET, ethanol.

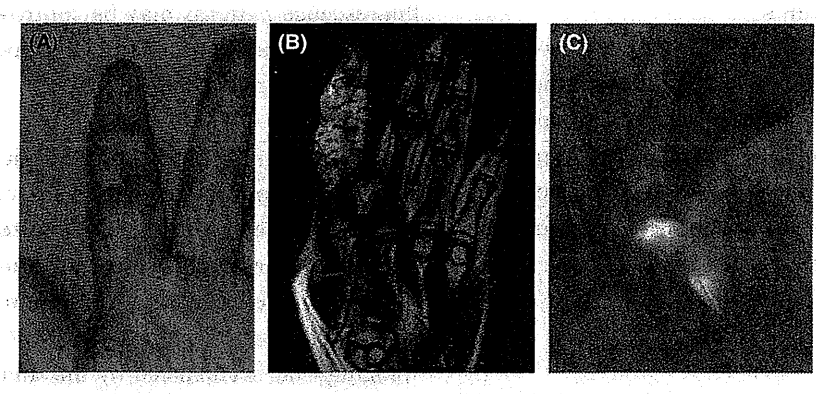

Figure 1. Case 14. Patient with venous malformation in the left index finger. (A) Preoperative view of the left hand. (B) Coronal fat-suppressed T2-weighted magnetic resonance image obtained before sclerotherapy shows a homogenous hyperintense mass in the left index finger. (C) Fluorescence image obtained during sclerotherapy shows unilateral contrast of the treated region of the index finger. Sclerotherapy was stopped when fluorescence images were obtained at the contralateral side of the index finger.

were obtained from the skin surface in 13 of the 15 procedures (87%) and linear fluorescence images in eight (53%). No fluorescence images were obtained in two patients with intramuscular venous malformations in the lower extremities. These intramuscular lesions were located more than 1 cm below the skin surface. Image quality and spatial resolution on PDE were sufficient for visualization of ICG and sclerosant spread. In two procedures (patients 8 and 14), NIR fluorescence imaging was useful in deciding when to stop the sclerotherapy because fluorescence images were obtained at the contralateral side of the treated finger (Figure 1). Linear fluorescence images were more likely to be obtained in the upper extremities and the face than in the lower extremities (Table 2). Linear images seemed to represent the flow in draining vessels, and spotty images seemed to represent the intralesional or extralesional existence of ICG. Fluorescence images were obtained at the end of the procedure, which

TABLE 2. Evaluation of Pattern of Fluorescence Images in 15 Patients

Distribution of Venous Malformations	Pattern n		
	Linear Images	Spotty Images	None Obtained
Upper extremity	4		
Lower extremity	1	4	2
Face	3	1	

took approximately 30 minutes, without a decrease in fluorescence. No worsening of the initial clinical situation occurred, and no complications associated with ICG were observed. The volume of ethanol used per treatment session ranged from 0.8 to 36.2 mL (average 14.3 mL) and that of foam polidocanol from 4.0 to 19.8 mL (average 8.5 mL). A local complication occurred as a result of the procedure in one of the 15 procedures. Intraoral ulceration occurred in a 17-year-old man (patient 2) with an extensive venous malformation of the face who had undergone ethanol sclerotherapy of the lip but eventually healed. No other complications, such as cutaneous necrosis, damage to local nerve, and symptomatic embolism of the sclerosant into the circulation, were observed during follow-up.

Discussion

Percutaneous sclerotherapy has been established as a minimally invasive treatment option for slow-flow vascular malformations.[2] The combination of sonographic and fluoroscopic guidance increases the safety of the procedure by allowing direct imaging of venous drainage.[3] Duplex sonography has been described as a real-time guidance technique providing visualization of the extent of the malformation and assessment of blood flow velocity.[4] MR-guided sclerotherapy allows direct visualization of needle placement and sclerosant distribution.[5] The value of navigation guidance for percutaneous sclerotherapy is based on the additional information derived from visualization of the target lesion. Several recent investigational studies have used NIR fluorescence imaging system after administration of ICG for intraoperative identification of lymph nodes and patency of lymph and blood vessels, as well as noninvasive assessment of lymphatic function.[6,11]

Duplex-guided sclerotherapy has been our standard method for the treatment of venous malformations. In this trial, we used real-time NIR fluorescence imaging as an additional monitor of the spread of sclerosant intraoperatively. Although observation on duplex sonography is limited to the cross-sectional area contacted by the probe, NIR fluorescence imaging can visualize sclerosant spreading horizontally on the skin surface. Nevertheless, extravasation of the ICG–sclerosant solution may cause visualization of extravascular space. Given that ICG binds to globulin proteins within tissues, it may be taken up by the lymphatics and visualize lymphatic vessels unexpectedly. Visual interpretation of the spotty fluorescence patterns may be controversial if they reflect intravascular spread or extravasation of sclerosant in this series.

Owing to its sensitivity, fluoroscopic imaging with radiopaque contrast medium is the clinical standard for vascular imaging, but NIR fluorescence imaging may provide noninvasive visualization that can be repeatedly excited without radiation exposure. There is also an advantage for NIR fluorescence imaging that is enhanced by the smaller amounts of contrast agent than with MR- or computed tomography–based angiography procedures.[6] Depth of penetration of NIR fluorescence is estimated to be between 2 and 3 cm below the skin surface.[7] In this series, observational depth seemed to be <1 cm below the skin surface with an ICG concentration of 0.01 mg/mL.

For sclerotherapy of venous malformations, especially those in the face and hands, the risk of necrosis should be carefully considered from an esthetic point of view. Linear fluorescence images were obtained more often in these regions (Table 2), because it was assumed that subcutaneous tissue was thin and vascular vessels well-developed.

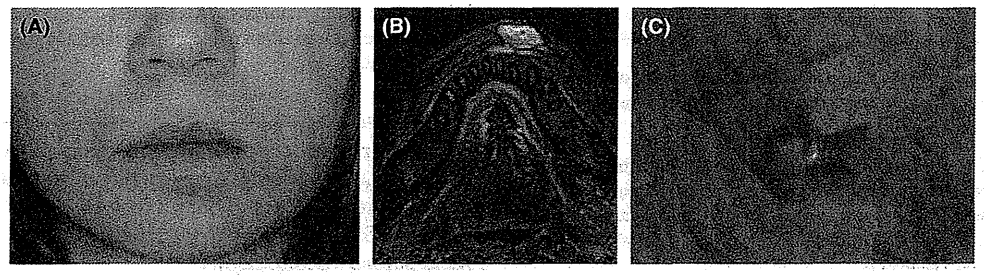

Figure 2. Case 15. Patient with venous malformation in the lower lip. (A) Preoperative view of the face. (B) Axial fat-suppressed T2-weighted magnetic resonance image obtained before sclerotherapy shows a homogenous hyperintense mass in the lower lip. (C) Fluorescence image obtained during sclerotherapy shows the spread of sclerosant in the lower lip.

Because of the limits of its tissue-penetrating depth, NIR fluorescence imaging can be suitable for lesions located in the face and hands (Figures 1 and 2). For lesions located in the fingers, the flow of sclerosant to the contralateral side of the treated finger could lead to total necrosis of the finger. In duplex-guided sclerotherapy, it is difficult to monitor the spread of sclerosant in the whole finger. NIR fluorescence imaging made it possible to detect flow to the contralateral side of the treated finger.

ICG is a tricarbocynanine dye that has been used clinically for longer than 50 years for hepatic clearance, cardiovascular function testing, and retinal angiography on the basis of its dark green color. ICG associates with albumin, making it an excellent vascular agent for evaluating the blood and lymphatic systems.[6] Most studies have used NIR fluorescence imaging systems after administration of mg amounts of ICG.[6,11] Our ICG concentration of 0.01mg/mL was enough to get visualization of sclerosant spreading. The incidence of adverse reactions related to ICG injection was reported to be 0.4%, and 0.05% for severe adverse reactions such as hypotension, arrhythmia, and anaphylactic shock.[12] No suspended matter was found in the mixture of ICG with absolute ethanol or 3% polidocanol, and the mixed solution was stable.

NIR fluorescence images with ICG were obtained in 13 of 15 procedures (87%) without any complications associated with ICG. This technique of NIR fluorescence imaging is safe and noninvasive. The device is portable and easy to use, and real-time fluorescence images can be obtained. The combination of duplex sonography and NIR fluorescence imaging may provide safer, more-efficient sclerotherapy. Although further study is necessary to validate the results of this trial, this method can be used as a useful additional monitor for sclerotherapy of venous malformations, especially those located in the face and hands.

References

1. Yakes WF, Haas DK, Parker SH, Gibson MD, et al. Symptomatic vascular malformations: ethanol embolotherapy. Radiology 1989;170:1059–66.
2. Berenguer B, Burrows PE, Zurakowski D, Mulliken JB. Sclerotherapy of craniofacial venous malformations: complications and results. Plast Reconstr Surg 1999;104:1–11.
3. Donnelly LF, Bissett GS 3rd, Adams DM. Combined sonographic and fluoroscopic guidance: a modified technique for percutaneous sclerosis of low-flow vascular malformations. AJR Am J Roentgenol 1999;173:655–7.
4. Yamaki T, Nozaki M, Sasaki K. Color duplex-guided sclerotherapy for the treatment of venous malformations. Dermatol Surg 2000;26:323–8.
5. Hayashi N, Masumoto T, Okubo T, Abe O, et al. Hemangiomas in the face and extremities: MR-guided sclerotherapy-optimization with monitoring of signal intensity changes in vivo. Radiology 2003;226:567–72.
6. Marshall MV, Rasmussen JC, Tan I-C, Aldrich MB, et al. Near-infrared fluorescence imaging in humans with indocyanine green: a review and update. Open Surg Oncol J 2010;2:12–25.
7. Kikuchi M, Hosokawa K. Visualized sclerotherapy of varicose veins. Dermatol Surg 2010;36(Suppl 2):1050–5.
8. Meyer JS, Hoffer FA, Barnes PD, Mulliken JB. Biological classification of soft-tissue vascular anomalies: MR correlation. AJR Am J Roentgenol 1991;157:559–64.

9. Benson RC, Kues HA. Fluorescence properties of indocyanine green as related to angiography. Phys Med Biol 1978;23:159–63.

10. Tessari L, Cavezzi A, Frullini A. Preliminary experience with a new sclerosing foam in the treatment of varicose veins. Dermatol Surg 2001;27:58–60.

11. Furukawa H, Osawa M, Saito A, Hayashi T, et al. Microsurgical lymphaticovenous implantation targeting dermal lymphatic backflow using indocyanine green fluorescence lymphography in the treatment of postmastectomy lymphedema. Plast Reconstr Surg 2011;127:1804–11.

12. Hope-Ross M, Yannuzzi LA, Gragoudas ES, Guyer DR, et al. Adverse reactions due to indocyanine green. Ophthalmology 1994;101:529–33.

Address correspondence and reprint requests to: Satoru Sasaki, MD, PhD, Center for Vascular Anomalies, KKR Sapporo Medical Center Tonan Hospital, Kita 1, Nishi 6, Chuou-ku, Sapporo 060–0001, Japan, or
e-mail: satoru-s@tonan.gr.jp

Journal of Tissue Viability (2013) 22, 103–111

JOURNALOF tissueviability

www.elsevier.com/locate/jtv

Review

Vascular anomalies and wounds

Sadanori Akita*, Seiji Houbara, Mihoko Akatsuka, Akiyoshi Hirano

Department of Plastic Surgery, Nagasaki University Hospital, 1-7-1 Sakamoto, Nagasaki 8538501, Japan

KEYWORDS
Vascular anomaly;
Vascular tumour;
Vascular malformation;
Ulcer;
Necrosis

Abstract Vascular anomalies comprise vascular tumours and vascular malformations. Some vascular anomalies result in ulcerations and necrosis. In vascular tumours, infantile haemangiomas are predominant and ulceration is demonstrated in up to 16%. In vascular malformations, arteriovenous malformations predominate and frequently demonstrate either primary ulceration or skin necrosis after diagnostic and therapeutic procedures. Various diagnostic and therapeutic imaging methods, such as X-ray, computed tomography (CT), magnetic resonance imaging (MRI), duplex Doppler ultrasound, and angiography, are used to visualize vascular anomalies; angiograms are required when embolization is attempted and blood flow needs to be further investigated. Duplex Doppler ultrasound is useful for routine check-ups as a therapeutic tool; however, it has limited in precision and accuracy. The aim of the present review is to give an overview of wounds related to vascular anomalies, detailing the diagnostic imaging and treatment options.

Introduction

Vascular anomalies comprise two distinct main types: vascular tumours and vascular malformations. Vascular malformations include capillary malformation (CM), venous malformation (VM), lymphatic malformation (LM), and arteriovenous malformation (AVM) [1], and are distinct from vascular tumours regarding clinical appearance, imaging, and histopathological characteristics [2]. Vascular tumours mainly comprise infantile haemangioma (IH) and other related rare vascular tumours, such as congenital haemangiomas (rapidly involuting congenital haemangioma, RICH or non-involuting congenital haemangioma, NICH), kaposiform haemangioendothelioma, tufted angioma, pyogenic granuloma, and haemangiopericytoma in children and in adults.

Various imaging methods, such as ultrasound, magnetic resonance imaging (MRI), computed tomography (CT), and angiography, are employed in the diagnosis of vascular tumours and vascular malformations. The selection of these techniques is based on the clinical findings and the aim of imaging, i.e., diagnostic, pre- and intra-treatment assessment, or follow-up.

The present review reflects the authors' experience with from January 2006 to March 2012, in which 231 cases of vascular anomalies (201 cases

* Corresponding author.
E-mail address: akitas@hf.rim.or.jp (S. Akita).

0965-206X/$36
http://dx.doi.org/10.1016/j.jtv.2013.08.001

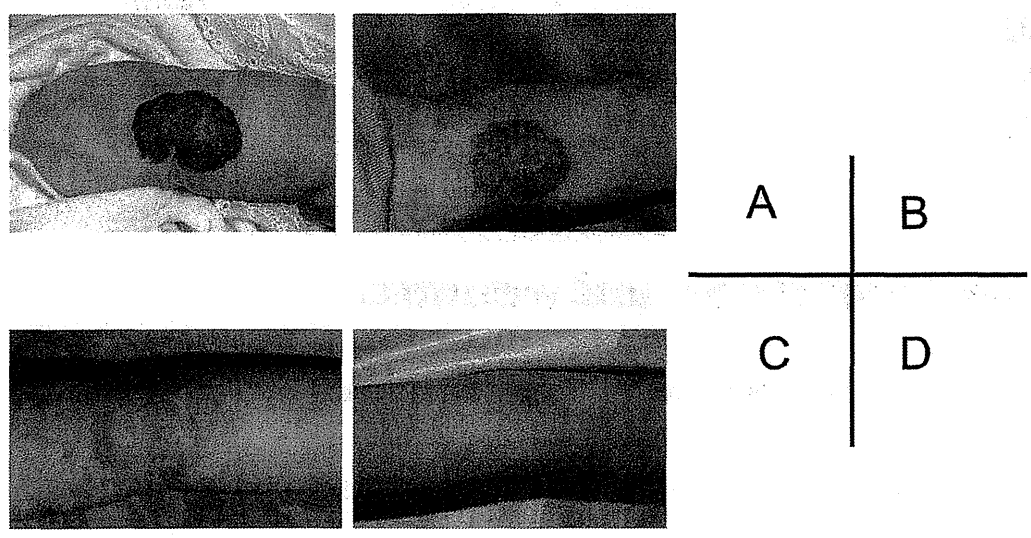

Figure 1 Typical IH in the elbow. A: At 4 months old, appearance of the lesion at the first visit. B: At 1.5 years of age, the redness has decreased. C: At 2.5 years of age, the colour has become much fainter. D: At 6 years of age, the colour has completely regressed and the skin shows some anetoderma. (For interpretation of the references to colour in this figure legend, the reader is referred to the web version of this article.)

were vascular malformations and 30 cases were haemangiomas) were treated in the Department of Plastic and Reconstructive Surgery, Nagasaki University Hospital. Among the cases of vascular malformations, the number of patients with VMs, AVMs, LMs, lymphatico-venous malformations (LVMs), capillary malformations (CMs), capillary-venous malformations (CVMs), arteriovenous-lymphatic malformation (AVLMs) was 114, 43, 17, 9, 9, 5, and 4, respectively. Of the haemangiomas, 28 cases were IHs and two were congenital haemangiomas (mean age: 32.6 ± 22.76; range; 3 months to 88 years). There were seven cases of primary ulceration in 201 vascular malformations and two in 30 cases of haemangiomas. All treatments in this clinical series were approved by the Internal Review Board of Nagasaki University (approved number 10032690) and informed consent was obtained.

IH

The majority of IHs are small and not hazardous, may recede spontaneously with proliferation, involution, and involuted phases. IH can be alarming if they occur at life- and function-threatening locations, such as the eyelid, orbit,

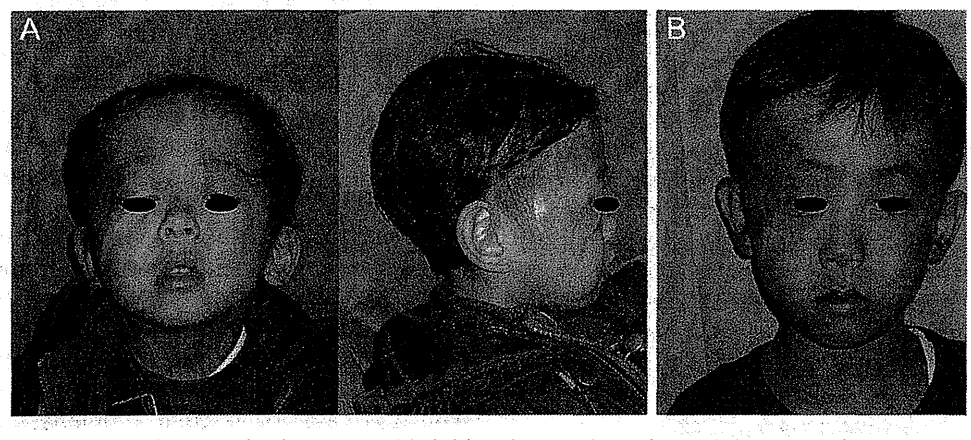

Figure 2 Healed IH. A: Photograph of a 2-year-old child with IH in the right eyelid, temporal area, and cheek, which shows laxity and shrinkage of the skin overhanging the eye at first visit. B: At 6 years after surgical removal of the lax skin and anetoderma.

Figure 3 NICH in a child at 7 months (left) and at 4 years of age (right). Clinical manifestations remained over the 3-year period.

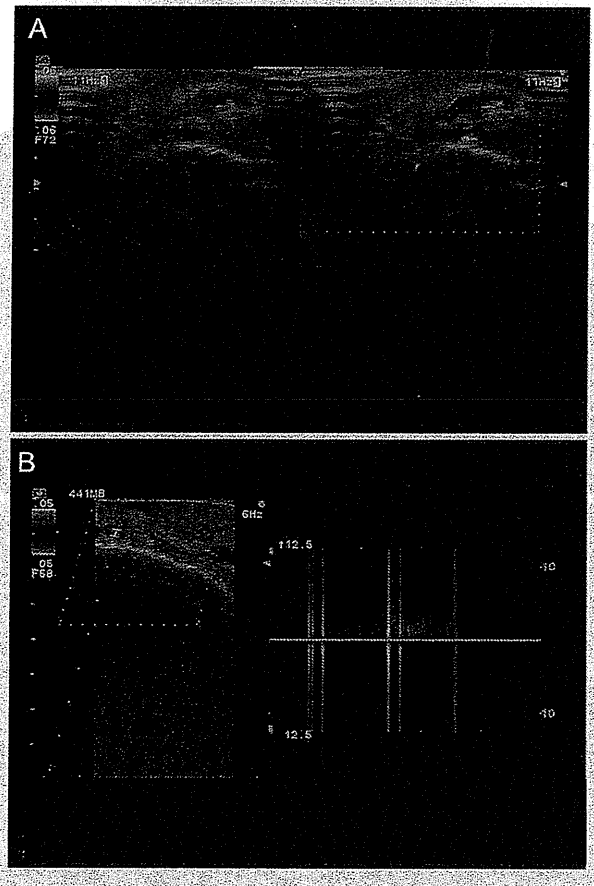

Figure 4 Duplex Doppler ultrasound. A: In-flow view, the hypervascularity of in- and out-flows is observed, as frequently seen in AVMs (arrow). B: Doppler mode demonstrates fast shunt flow. Progression of IH in the left elbow joint at 4 months in the first visit (left) and at 6 years (right).

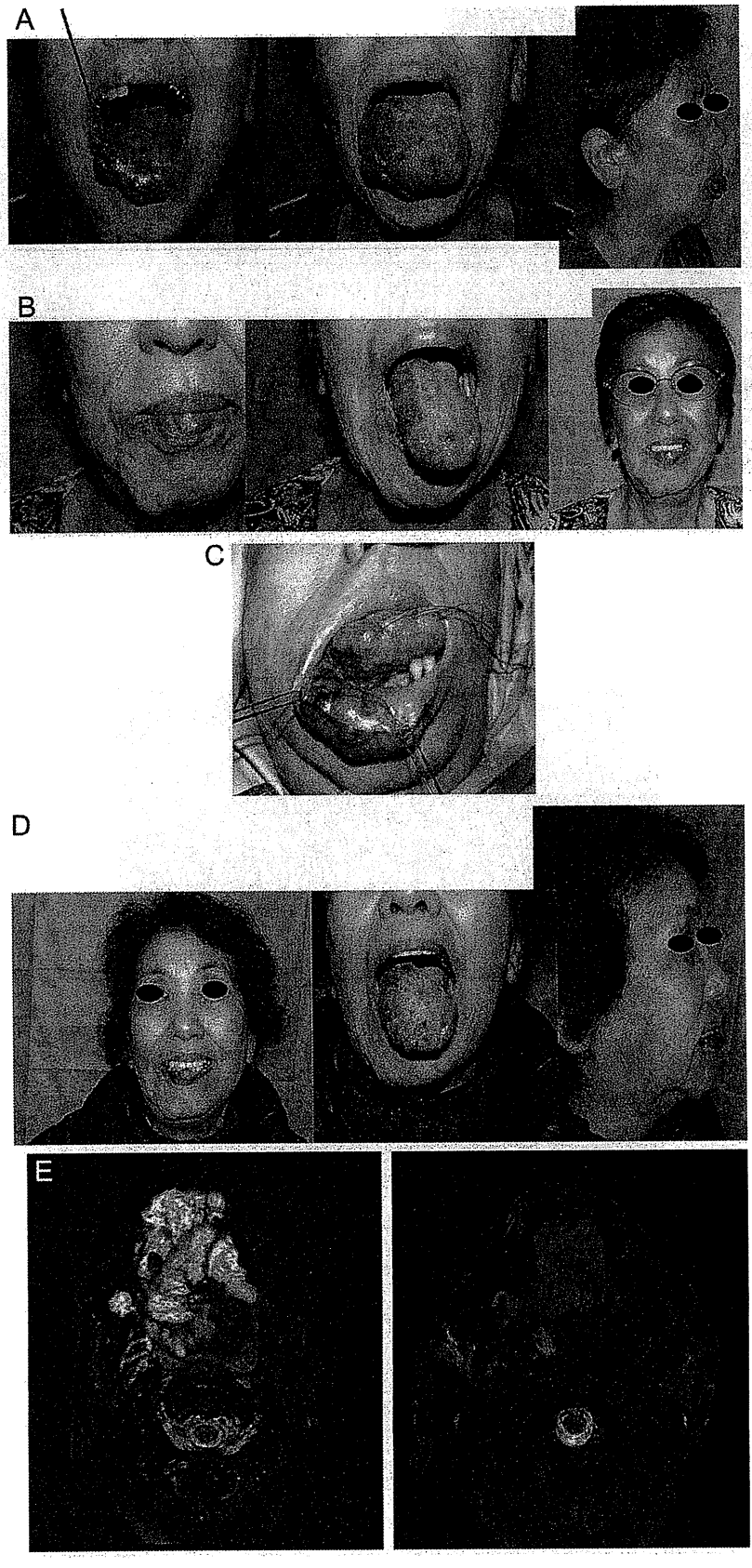
A
B
C
D
E

or airway. In those cases involving ulceration, continued infection, or haemorrhage treatment is required. Ulceration is one of the most common complications of IH. The incidence in a referral population is generally reported to be approximately 16%. A prospective study of 1096 patients reported the median age at ulceration was 4 months, which correlates with the end of the proliferative phase [3]. Risk factors for ulceration include segmental morphological characteristics, large size, and mixed superficial and deep subtypes. Early white discolouration may suggest impending ulceration [4]. In ulcerated IH, initial chemotherapy comprising 2 mg/kg β-blockers daily until 6 months after wound healing resulted in complete wound healing and marked involution in a 3 year-old girl [5].

Vascular malformations

Vascular malformations consist of CM, VM, LM, and AVM. Combinations of more than one malformation are categorized as complex vascular malformations and complex syndromes, such as Klippel—Trénaunay syndrome (CM + VM + LM) or Parkes Weber syndrome [AVM/or arteriovenous fistula (AVF) + skin pseudo-CM + lymphoedema], which presents with more systemic signs and symptoms. Skin necrosis often manifests in severe AVM, combined CM + LM, and a minority of cases of IH.

Assessment and imaging tools

Many imaging tools are able to determine the diagnosis of vascular malformations; however, relevant clinical signs and manifestations are also sought to enable a definitive diagnosis. Less invasive methods are usually applied first, but it is very important to evaluate the vascularity and dynamic changes using angiography in AVMs.

Conventional X-rays

Radiography is usually of little or no value in most cases. VMs may be diagnosed if phleboliths (vascular stones) are observed on plain X-rays. Bone distortion is only seen in large malformations with a soft-tissue mass effect. Some diffuse and massive VMs cause osteolytic lesions and generate a risk of pathological fractures. AVMs involving bone sometimes lead to osteolytic lesions due to intra-osseous nidus formation, which forms owing to arteriovenous shunting or large draining venous channels after the nidus.

Duplex Doppler ultrasonography

Duplex Doppler ultrasonography is primarily used as the initial diagnostic tool [6]. It permits distinction between vascular tumours and malformation, and it also provides information regarding anatomical location. It demonstrates that the lesion is either cystic or tissular, clarifies the presence or absence of flow, and thus, distinguishes between fast-flow and slow-flow malformations, as well as intensity and direction of the flows. Angiostructure and vessel density can be assessed; however, frequently with poor reliability. Peak flow velocities and arterial output may be measured in AVMs. In a head and neck or an extremity AVM, comparing arterial output on the normal side with the abnormal contralateral side is crucial in prognosis, especially possible cardiac failure, and is thus useful for follow-up of AVMs.

CT

CT is of limited use, even after enhancement using intravenous iodinated contrast media; the information provided is limited to indicating whether a lesion is highly vascularized or not. Precise delineation and diagnosis of soft-tissue lesions remain poor with the exception of macrocystic LMs, whereby cysts are clearly depicted. The presence of phleboliths may lead to a diagnosis of VM as distinctive calcifications develop on thrombosis and debris as a result of slow flow. Bony displacement or alteration can be seen due to chronic (long-term) compression, which is seen in both VMs and LMs. Pathological fractures and absorption may be seen in bone or bone-adjacent AVMs.

Figure 5 VMs in the face and neck. A: A 62-year-old woman with VM in the face and neck (lip, tongue, oral floor, neck). Arrow indicates ulceration due to the tight contact with the swollen oral cavity and lip (vermillion). B: At 6 months after the second course of ultrasonic-guided sclerotherapy using absolute ethanol. C: At the third course of sclerotherapy, the excessive tissue was surgically removed. D: At 2 years, after the third course of sclerotherapy and surgery. E: Change of VM is visualized using T2-weighed MRI.